Turkish Journal of Civil Engineering, 2024 47-70, Paper 769, ***Research Article***

Protection of Reinforced Concrete Columns from Pounding-Induced Effects in Adjacent Buildings

Sueda ALTAN OYMANLI[1*]
Özgür AVŞAR[2]

ABSTRACT

The pounding damage is one of the most common seismic damage types observed after past earthquakes in adjacent reinforced concrete (RC) buildings having insufficient gap in-between. Particularly in highly populated regions, there are numerous adjacent RC buildings, in which pounding can cause severe damage or total collapse. Many previous reconnaissance reports following earthquakes have emphasized severe column damage due to pounding with the slab of adjacent building. In this paper, a retrofitting method is presented to reduce the seismic damage caused by pounding on existing RC structural elements in cases where collision is unavoidable. Pounding effects are investigated by using 4- and 7-story RC buildings with unequal floor elevations. As a retrofitting solution for pounding, steel columns and neoprene rubber pads are placed at the mid-height of the story so that the pounding takes place between the neighbouring slab and added steel columns instead of existing RC columns. The mid-column pounding of existing RC buildings with and without retrofitting are numerically investigated. In the numerical model, buildings are connected by link elements to produce the pounding in-between. Nonlinear response history analyses are performed using 11 different real ground-motion records. Pounding forces, peak floor accelerations, inter-story drift ratios, story shear force distributions, and plastic hinge distributions are obtained and compared for each of the pounding conditions. The analysis results reveal that the proposed retrofitting method protects the existing RC columns from brittle type of shear failure and reduces the destructive effects of pounding.

Keywords: Pounding, seismic damage, retrofitting, adjacent buildings, reinforced concrete, link element.

Note:
- This paper was received on April 10, 2023 and accepted for publication by the Editorial Board on December 22, 2023.
- Discussions on this paper will be accepted by July 31, 2024.
- https://doi.org/10.18400/tjce.1280691

1 Eskisehir, Türkiye
sueda.altan19@gmail.com - https://orcid.org/0000-0001-8872-0544

2 Eskisehir Technical University, Department of Civil Engineering, Eskisehir, Türkiye
ozguravsar@eskisehir.edu.tr - https://orcid.org/0000-0001-7246-9631

* Corresponding author

1. INTRODUCTION

Earthquakes are one of the most common natural disasters that result in loss of life and property in the seismically active regions. Adjacent buildings can collide due to the insufficient seismic gap between them or due to their out-of-phase vibrations [1,2].

This phenomenon is referred to as pounding, which is one of the common causes of damage observed during earthquakes. Especially in metropolitan cities, there are numerous buildings with insufficient seismic gap between them, and these adjacent buildings are under the risk of structural damage due to pounding in future earthquakes. Therefore, it is necessary to minimize the risks arising from earthquake-induced pounding damage.

Leaving sufficient seismic gaps ensuring that a collision does not occur between adjacent buildings is the most effective method for preventing the occurrence of pounding. Therefore, a minimum seismic gap that shall be placed between two buildings has been specified to avoid pounding in building design codes. In the Turkish Building Earthquake Code (TBEC-2018) [3], the minimum size of gap shall not be less than the value obtained by multiplying the coefficient (α) by the square root of the sum of squares of displacements obtained in adjacent buildings for each floor. If all floor levels of adjacent buildings are the same at all stories, the coefficient (α) is 0.25R/I; otherwise, the coefficient is 0.5R/I. R and I represent the structural system behaviour factor and importance factor, respectively. In addition, gap distance shall not be less than 30 mm up to 6.0 m height and shall be increased by 10 mm for each additional 3.0 m above 6.0 m and shall be arranged to allow independent movement of building blocks in all earthquake directions. In some studies, the adequacy of the seismic gap specified in building codes is investigated [2,4]. There are other studies conducted to determine the minimum seismic gap required to prevent a collision [5-9].

Mostly, during the construction stage, the seismic gap calculated according to the earthquake design code requirements is neither considered nor inspected properly between adjacent buildings.

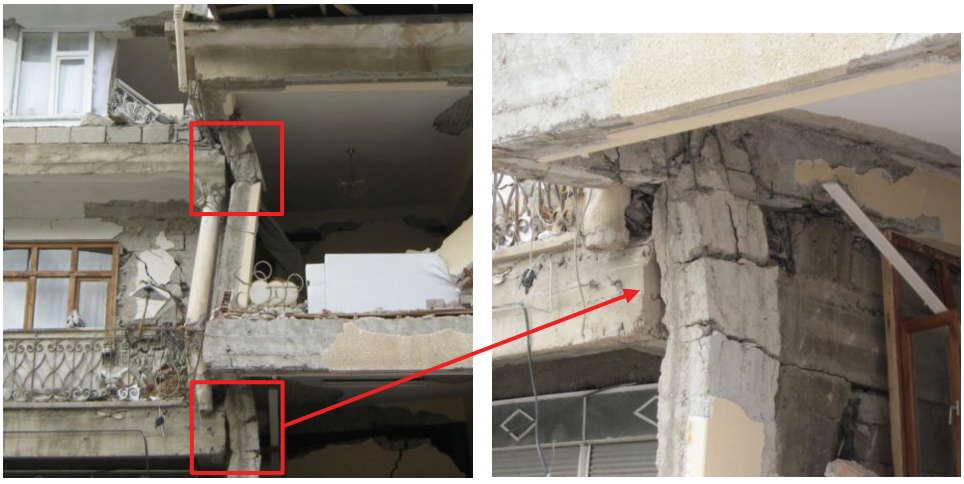

Fig. 1 – Examples of Pounding failures. [13]

The collision between buildings can cause local damages or total collapse. Slab to column collision is much more critical due to large shear forces imposed on the columns as a result of pounding [10-12]. The shear capacity of the columns can be exceeded as a result of the impact of the adjacent slab that has very high in-plane stiffness and capacity. As a result, occurrence of column shear damage can lead to partial or total collapse of the buildings as shown in Fig. 1.

Pounding has been observed in many past earthquakes. Following the 1985 Mexico City Earthquake, it was reported that 40 percent of the buildings collided with each other, and pounding damages were observed in 15 percent of the severely damaged buildings [14]. The same phenomenon was observed in Loma Prieta Earthquake (1989), which affected over 500 buildings and caused pounding damage in over 200 buildings [15]. After the 1999 Kocaeli Earthquake in Turkey, severe column damage was reported as a result of a collision between a six-story building and a two-story neighbouring building [16]. Following the earthquake, reconnaissance studies and reports revealed that the pounding caused significant damage to the RC buildings [17–21]. Many experimental and numerical studies have also show that pounding affects the seismic behaviour of buildings [22-29].

Thus, retrofitting methods to avoid the pounding have been the topic of many previous studies.

Anagnostopoulos [30] proposed the placement of impact-absorbing materials between the reinforced concrete structures to reduce the pounding effects. Many studies investigated the effect of use of impact-absorbing materials on the response of colliding buildings [31-35].

Using supplemental energy dissipation devices reduces the maximum lateral displacements of the building. However, such supplemental energy dissipation devices may not be sufficient to prevent pounding in all conditions. Structural pounding can be avoided by increasing the stiffness of the buildings using shear walls and bracing systems [36,37]. Shear walls reduce the lateral displacements by increasing the stiffness of the building. If the displacements could not be sufficiently reduced to the point where the collision is prevented, pounding is inevitable and existing frame elements that collide with the adjacent building will be severely damaged. Another mitigation measure proposed in the literature is to connect adjacent buildings with links to keep structural vibrations in phase without causing pounding [38,39]. Abdel-Mooty and Ahmed [40] proposed a retrofitting solution using localized interconnections between adjacent parts of the structure. In this case, seismic damage is especially localized in the connection points of these link elements at existing building components. Fluid viscous dampers and friction dampers have also been used to mitigate the pounding effects in adjacent buildings [41]. Pargoo et al. [42] suggested implementing viscous wall dampers in adjacent structures to reduce the pounding-induced effects.

Many studies have indicated that the most efficient method of preventing pounding is to leave a sufficient gap between the buildings or to upgrade the stiffness of the structural system by introducing structural walls in order to minimize the structural displacements to avoid pounding. The adequacy of the proposed retrofitting methods in terms of preventing pounding phenomenon includes several uncertainties such as the approximations in calculating the inelastic displacements. However, there is no retrofitting method or published study for preventing pounding-induced structural damage for existing buildings that have already been constructed without sufficient seismic joint, and where pounding is

unavoidable. This study aims to minimize the seismic damage caused by pounding on existing RC structural elements in cases where collision is unavoidable. For this purpose, existing adjacent RC buildings are retrofitted with steel columns and neoprene rubber pads which are added to the existing structural system of buildings. Therefore, pounding will take place between the added steel columns and the slab of the adjacent building. By this retrofitting approach, existing RC columns can be protected by diverting the collision to the steel columns. Then the pounding forces will be transferred from the pin connected steel columns to the slabs, whose in-plane capacity is the largest compared to the capacity of any other structural component of the exiting substandard RC buildings. Like the capacity design principles adopted in the seismic design of buildings, the proposed retrofitting approach receives use of the capacity of the strongest link, which is the in-plane capacity of slabs, in the existing substandard RC building when pounding takes place.

2. PROPOSED RETROFITTING METHOD

The proposed retrofitting approach is intended to prevent column damage when pounding is unavoidable. In order to protect the existing RC columns from pounding effects, steel columns are placed at each story of the buildings by partially removing the infill wall and pounding is ensured in these elements instead of existing substandard RC columns. Steel columns added to the structural system of the buildings are shown in Fig. 2. The additional steel columns are placed such that the pounding first takes place with them by extending steel beam elements at the pounding level. Therefore, added steel columns by means of the proposed retrofitting approach can only be effective in the case of floor-to-column pounding.

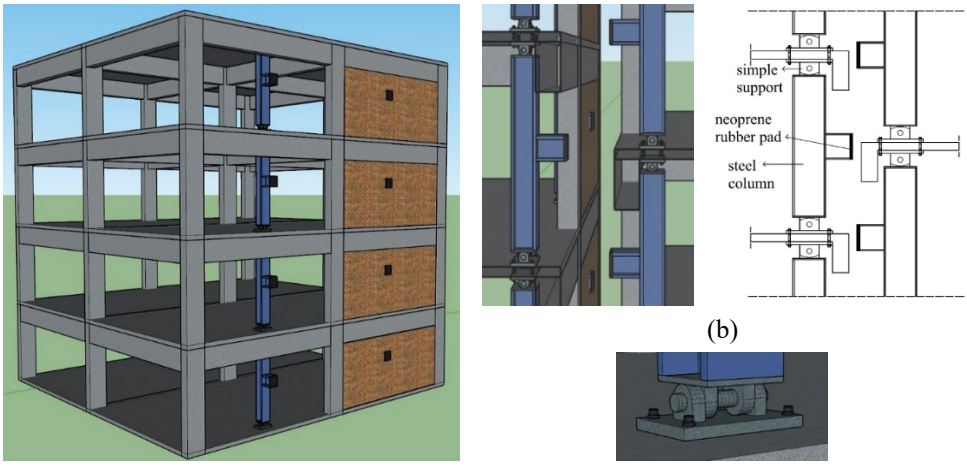

Fig. 2 - (a) Proposed retrofitting method, (b) sectional view of columns, (c) connection detail.

The steel columns are connected to the floor with a simple support at both ends (Fig. 2(c)). With this connection detail, only axial loads are transferred to the floors where the steel column is supported. The floors that have very high in-plane stiffness and capacity distribute the impact forces to the vertical structural members in accordance with their stiffness. Furthermore, neoprene rubber pads are placed on the steel columns to provide additional damping in the system during the collision and to prevent local damage that may occur on steel columns and the concrete slab.

3. BUILDING FEATURES AND MODELING

3.1. Properties of Adjacent Buildings

Low and mid-rise RC buildings constitute a significant portion of Turkey's existing building stock. Therefore, the study focused on 4- and 7-story RC buildings that represent typical members of the existing building stock. Building models are determined from an inventory study that is investigated about 500 RC buildings by Inel et al. [43]. 4- and 7-story buildings are designed according to previous seismic codes. The reason for selecting these two RC buildings is that the pounding phenomenon can take place due to their different dynamic characteristics ensuring that their vibration modes will not be in phase and pounding can take place in between.

Buildings have RC frame system constituted by beams and columns with no structural wall. Plan view of ground story for both buildings is shown in Fig. 3. In both buildings, the sizes of the structural system elements are smaller at the upper floors. The column and beam dimensions of 4- and 7- story buildings are given in *Table 1*.

4-story building has a total length of 15 m in the x-direction, 10 m in the y-direction. 7-story building has a total length of 19.5 m in the x-direction, 13 m in the y-direction. Story heights in both building models are 2.8 m. In the design of both buildings, as per TBEC-2018, the importance factor of both buildings and the soil class is taken as “1” and ZC (very dense sand, gravel, or very stiff clay), respectively.

Concrete compressive strength of both building models is 16 MPa. Nominal yield strength of both longitudinal and transverse reinforcements of 4- and 7-story buildings are 420 MPa and 220 MPa, respectively.

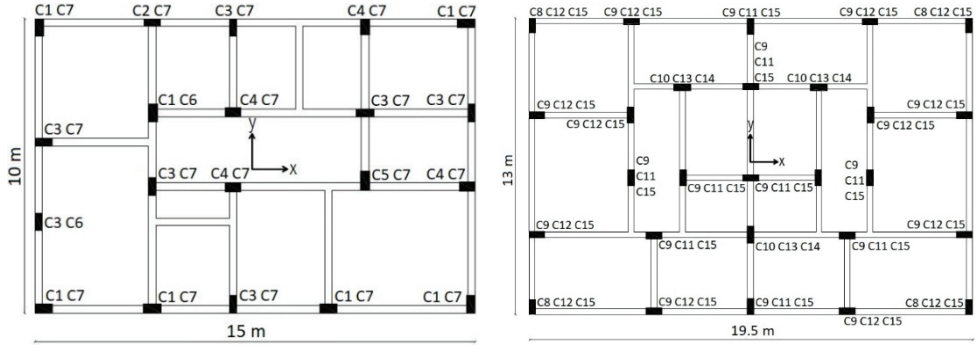

(a) (b)

Fig. 3 - Plan view of ground story for buildings (a) 4-story, (b) 7-story.

Table 1 - The column and beam sizes of 4- and 7- story buildings.

Building model	Story level	Column label	Column size (cm)	Beam size (cm)
4-story	from 1 to 2	C1	30×60	25×60
		C2	25×55	
		C3	25×60	
		C4	30×55	
		C5	30×65	
	from 3 to 4	C6	25×50	
		C7	25×55	
7-story	from 1 to 2	C8	30×65	25×60
		C9	30×70	
		C10	30×75	
	from 3 to 4	C11	30×60	
		C12	25×60	
		C13	30×70	
	5	C11	30×60	25×50
		C12	25×60	
		C13	30×70	
	from 6 to 7	C14	30×60	
		C15	25×50	

Steel columns that are placed in the mid-bays on the collision surface of RC buildings are made of S235 (structural steel with a nominal yield strength of 235 MPa). Columns section is HE500M of standard European sections. Neoprene rubber pads have dimensions of 200×200×25 mm. The nominal hardness of the rubber bearings is 60 on the Shore A scale, which has the shear modulus, G of 1.1 MPa. The design of all components of the retrofitting scheme including the connection details to the RC slab is made such that they will not be exposed to any seismic damage under the impact forces during collision.

3.2. Nonlinear Modeling of Buildings

Three dimensional numerical models are developed for both buildings in SAP2000 [44]. The base of the columns is assumed to be fully restrained. Slabs are considered to be rigid diaphragms for the in-plane behaviour due to their larger cross-sectional area. The rigid diaphragm constraint is employed to reflect this behaviour of the slabs. In the nonlinear calculation method, effective stiffness coefficient values used for cracked sections of reinforced concrete sections are considered as per TBEC-2018.

Plastic hinges have been defined at both ends of columns and beams in reflecting non-linear behaviour in building models. P-M2-M3 plastic hinge is assigned for columns to consider the interaction between bi-axial flexure and normal force, whereas M3 plastic hinge is employed for beams. User-defined hinge properties are used in this study. The moment-plastic rotation relationship of the plastic hinges defined in the SAP2000 is given in Fig. 4. 'A', 'B', 'C', 'D', and 'E'. Moment-rotation relation of each plastic hinge are determined according to section geometry, material properties of reinforcement steel, confined and unconfined concrete, and axial load level on the RC members.

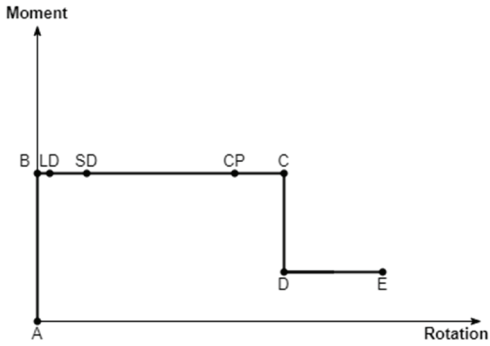

Fig. 4 - Moment-rotation relationship of the plastic hinge.

Mander's model is selected for concrete material models to define unconfined concrete and confined concrete [45]. Modulus of elasticity of concrete is taken as 20000 MPa according to TBEC-2018 for concrete class C16. The strain corresponding to the maximum strength of unconfined concrete is 0.002, the crushing strain is 0.0035, and the spalling strain is 0.005. The characteristics of the confined concrete model vary depending on the cross-sectional characteristics of the RC members and the detailing of the longitudinal and transverse reinforcement.

Two different grades of steel, which are S420 and S220, have been considered. Modulus of elasticity of reinforcement steel is taken as 200000 MPa. Yield strength, ultimate strength, failure strain, and yield strain values are given in *Table 2*.

Table 2 - Mechanical properties of reinforcement.

Reinforcement class	Yield Strength (MPa)	Ultimate Strength (MPa)	Yield Strain, ε_y	Failure Strain, ε_{su}
S220	220	264	0.0011	0.12
S420	420	550	0.0021	0.08

The moment-curvature relationship of the RC members is obtained using the cross-section analysis conducted in XTRACT [46]. The obtained moment-curvature values are used in the definition of plastic hinges to be lumped at critical sections of RC members. P-M2-M3

interaction and M3 hinges are assigned at the ends of columns and beams, respectively to identify the attainment of their capacities during the nonlinear analysis. The performance limits of Limited Damage (LD), Significant Damage (SD), and Collapse Prevention (CP) for the flexural hinges are specified from section analysis and the requirements of TBEC-2018. *Table 3* shows the damage levels for flexural response in terms of material strains specified in TBEC-2018. In the definition of moment-rotation relation, the plastic hinge length is considered to be the half of the section depth ($L_p = H/2$) as recommended in TBEC-2018.

Table 3 - Strain based damage levels as per TBEC-2018.

Damage Levels	Concrete Limit Condition	Steel Limit Condition
Limited Damage (LD)	$\varepsilon_c^{LD} = 0.0025$	$\varepsilon_s^{LD} = 0.0075$
Significant Damage (SD)	$\varepsilon_c^{SD} = 0.75\varepsilon_c^{CP}$	$\varepsilon_s^{SD} = 0.75\varepsilon_s^{CP}$
Collapse Prevention (CP)	$\varepsilon_c^{CP} = 0.0035 + 0.04\sqrt{\omega_{we}} \leq 0.018$	$\varepsilon_s^{CP} = 0.40\varepsilon_{su}$

where ε_c is concrete compressive strain, ε_s is the steel strain and ε_{su} steel strain at the maximum tensile stress and ω_{we} is the ratio of mechanical reinforcement of the effective stirrup. ω_{we} is calculated according TBEC-2018 as;

$$\omega_{we} = \alpha_{se}\rho_{sh,min}\frac{f_{ywe}}{f_{ce}} \tag{1}$$

$$\alpha_{se} = \left(1 - \frac{\sum a_i^2}{6b_o h_o}\right)\left(1 - \frac{s}{2b_o}\right)\left(1 - \frac{s}{2h_o}\right) \quad ; \quad \rho_{sh} = \frac{A_{sh}}{b_k s} \tag{2}$$

where α_{se} is the efficiency coefficient of transverse reinforcement, ρ_{sh} is volumetric ratio of transverse reinforcement, $\rho_{sh,min}$ is the minimum of the volumetric ratio of the transverse reinforcement in two horizontal directions, f_{ywe} is the yield strength of transverse reinforcement, f_{ce} is compressive strength of concrete, α_i is lateral distance between the axes of the longitudinal bars, which are supported by the transverse reinforcement, b_o and h_o are size of the cross-section between the axes of the transverse reinforcement of core concrete, s is the spacing of transverse reinforcement, A_{sh} is area of transverse reinforcement for rectangular section, b_k is cross section dimension of concrete core of column (distance between the centers or outermost rebars).

Shear hinges are also assigned to each frame member to determine whether its shear capacity has been attained during the analysis. Due to its brittle nature, only ultimate state limit is specified for the shear hinges assigned at the mid-span of the members to distinguish the shear hinges with the flexural hinges.

Flexural and shear hinges are assigned to steel columns placed on the pounding surface. In this way, the demands that will occur on the steel column are monitored. Plastic moment strength (M_p) and nominal shear strength (V_n) of steel columns are calculated according to Turkish Structural Steel Code [47] as follows;

$$M_p = F_y W_{px} \tag{3}$$

$$V_n = 0.6 F_y A_w C_{v1} \tag{4}$$

where F_y is the yield strength of structural steel, W_{px} is the plastic section modulus about x-axis, A_w is the area of the web, C_{v1} is the web shear strength coefficient, which is 1.0.

3.3. Examined Pounding Cases

Although there are buildings adjacent to the neighbouring building having the same floor elevations, the majority of the existing buildings are adjacent to the neighbouring building with different floor elevations. In this case, pounding takes place between the floor of one building and the columns of the other building. Story heights of both building models are 2.8 m. One of the buildings is moved in vertical direction in the numerical model so that pounding occurs in the mid-height of the columns. Slab-to-column collision models are established by connecting building models with link elements. Then, slab-to-steel column collision model is established by placing the steel columns in the mid-bays on the collision surface of 4-story and 7-story buildings. Moreover, individual 4-story and 7-story buildings where no pounding takes place are also examined for comparison purposes. Pounding models and link elements are presented in *Fig. 5*.

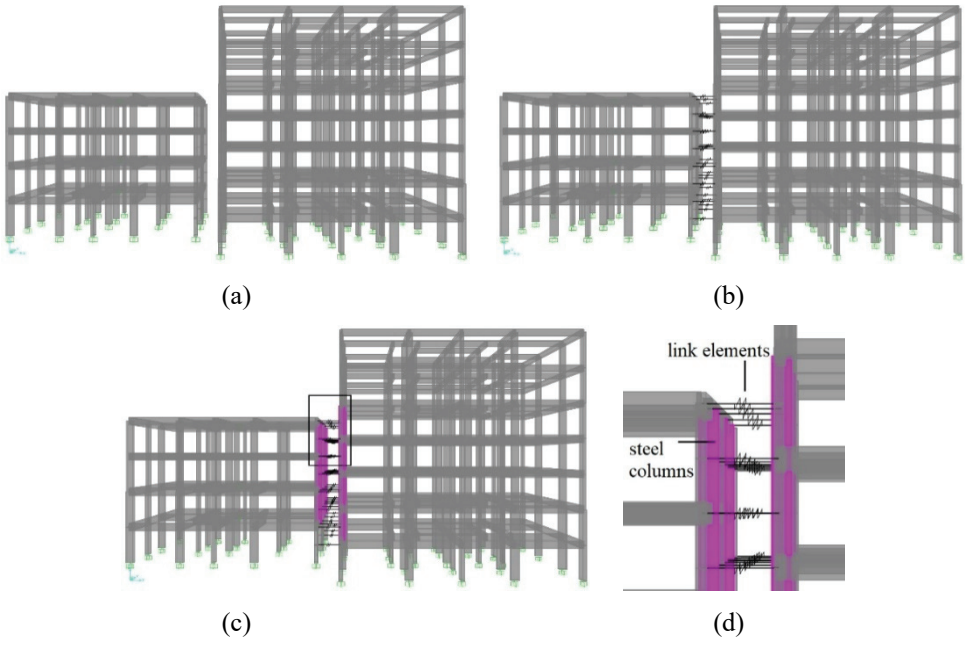

Fig. 5 - Pounding cases for (a) no collision, (b) pounding model of non-retrofitted buildings, (c) pounding model of retrofitted buildings, (d) link elements.

Several impact models are used to simulate the pounding between colliding buildings in literature [48–50]. Because of its simplicity and ease, the linear elastic spring model is commonly used in previous studies. In the linear elastic spring model, linear spring with a high stiffness is used to simulate impact once the gap between adjacent buildings closes. The spring is only activated when the calculated relative distance in the closing direction is greater or equal to the specified gap distance. In such a case, pounding takes place and spring stiffness becomes effective. The force-displacement relationship of a link element is shown in Fig. 6.. The impact force *F(t)*, based on linear elastic spring model is determined as follows;

$$F(t) = \begin{cases} k(\delta(t) - d), & \delta(t) - d > 0 \\ 0, & \delta(t) - d \leq 0 \end{cases} \tag{5}$$

$$\delta(t) = u_j(t) - u_i(t) \tag{6}$$

where k is the stiffness of the spring, $\delta(t)$ is the depth of interpenetration, $u_j(t)$ and $u_i(t)$ are the displacements of the two adjacent buildings and d is the gap distance.

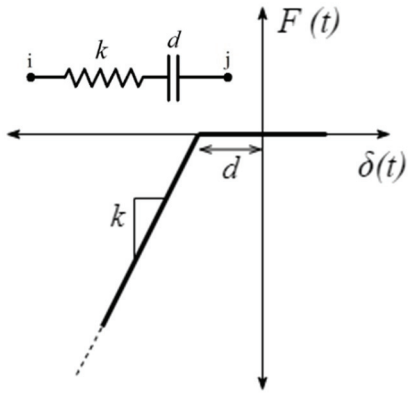

Fig. 6 - Force-displacement relationship for linear elastic spring model

The impact model is simulated by using nonlinear link element in SAP2000. When the gap distance closes during motion, the axial stiffness of the slab triggers in the stiffness matrix. The axial stiffness of the building's floor slab in the pounding direction is used to calculate the stiffness of the link element. The stiffness of link elements (k) is recommended to be greater than the axial stiffness of the slab of the adjacent buildings [30,51,52]. Based on the study of Altınel [53], the stiffness for the link elements is chosen as 35 times the axial stiffness corresponding to the effective area on the slab section where the pounding takes place. Hence k is calculated as;

$$k = \frac{EA}{L} \times 35 \tag{7}$$

where E is the modulus of elasticity of concrete, A is the effective cross-sectional area of the slab, L is the length of the slab in the direction perpendicular to the contact surface.

The gap distance between the adjacent buildings is defined in the link element. If pounding occurs, the gap distance is critical in the seismic response of both buildings. Although gap distance is variable in existing buildings, a constant gap distance of 40 mm is selected in this study to reflect an insufficient gap distance specified by TBEC-2018 to observe pounding. In order to make consistent comparisons, the same gap distance, 40 mm, is also considered in the retrofitted buildings, which includes steel columns and neoprene rubber pads. However, in real life applications of the proposed retrofitting approach, the additional steel column and neoprene rubber pad reduce the gap between the existing adjacent buildings.

The link elements defined in SAP2000 are used to model the neoprene rubber pad that will be added to the collision surface of the steel columns. The neoprene rubber pad is modeled as a spring connected in series to the link element. The axial stiffness of neoprene rubber pads adopted from Naeim and Kelly [54] calculated as follows:

$$K_v = \frac{E_c A}{t_r} \tag{8}$$

$$E_c = 6.73GS^2 \tag{9}$$

$$S = \frac{a}{4t} \tag{10}$$

where K_v is axial stiffness, E_c is elasticity modulus, A is the area of neoprene pad, t_r is the neoprene pad thickness, G is shear modulus, S shape factor, a is the side dimension of the square pad.

4. GROUND MOTION SELECTION AND SCALING

Real ground motion records obtained during earthquakes are used in nonlinear time history analyses. Recorded ground motions are selected and scaled with respect to the requirements of TBEC-2018. TBEC-2018 requires the selection of a minimum of 11 ground motion recordings, where at most three ground motion records can be selected from the same earthquake event. The selected ground motion records are scaled such that the average of the response spectra values should be greater than the ordinates of the TBEC-2018 target spectrum between the period range $0.2T_p$ and $1.5T_p$, where T_p is the natural period of the building model.

In this study, the PEER (Pacific Earthquake Engineering Research) strong ground motion database has been used for selecting the ground motion records (https://ngawest2.berkeley.edu/). Table 4 shows the main characteristics of the selected earthquake records. Since the analyses is performed along the x axis where the pounding takes place, only one of the horizontal components of the earthquakes is used. The component with the highest PGV value is chosen.

Table 4 - The properties of the selected earthquake records.

Record No	Earthquake Name	Station	Magnitude	Component	PGA (g)	PGV (cm/s)	PGD (cm)
RSN-879	Landers	Lucerne	7.28	260°	0.73	133.40	113.92
RSN-821	Erzincan, Turkey	Erzincan	6.69	NS	0.39	107.14	31.99
RSN-180	Imperial Valley-06	El Centro Array #5	6.53	230°	0.38	96.90	75.22
RSN-529	N. Palm Springs	North Palm Springs	6.06	210°	0.69	65.99	16.17
RSN-1602	Duzce, Turkey	Bolu	7.14	90°	0.81	65.88	13.10
RSN-959	Northridge-01	Canoga Park - Topanga Can	6.69	196°	0.39	63.29	13.17
RSN-183	Imperial Valley-06	El Centro Array #8	6.53	140°	0.61	54.49	41.78
RSN-1052	Northridge-01	Pacoima Kagel Canyon	6.69	360°	0.43	51.38	7.22
RSN-767	Loma Prieta	Gilroy Array #3	6.93	90°	0.37	45.43	24.11
RSN-727	Superstition Hills-02	Superstition Mtn Camera	6.54	135°	0.84	43.50	5.23
RSN-1165	Kocaeli, Turkey	Izmit	7.51	90°	0.23	38.29	24.29

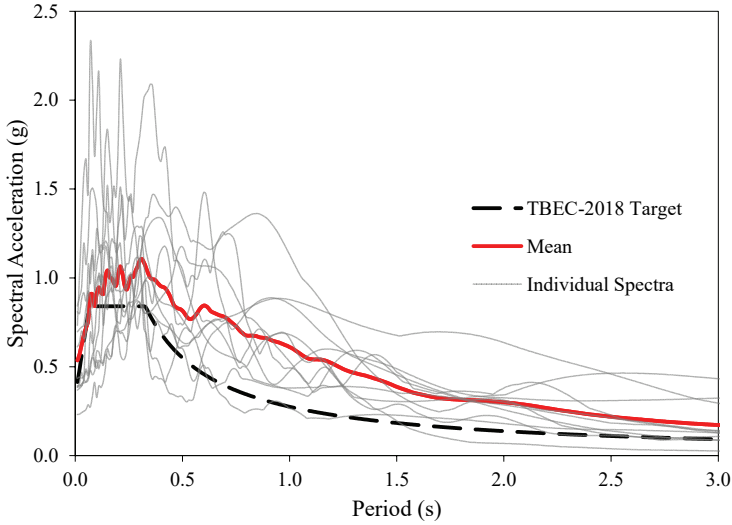

Fig. 7 - Elastic response spectra of the selected ground motion records.

The target design spectrum is defined by considering the coordinates, the soil type, and the earthquake ground motion level of the buildings. This information is used in the seismic hazard map of Turkey (https://tdth.afad.gov.tr) to obtain the design spectrum for the

investigated buildings. The target design spectrum corresponds to the seismic hazard level (DD-2) with 10 percent probability of exceedance in 50 years in TBEC-2018 for the specific location in Eskişehir city center with latitude coordinate of 39.763946°N and longitude coordinate of 30.514724°E. The soil type is ZC (very dense sand, gravel, or very stiff clay). *Fig. 7* shows the elastic response spectra of the selected ground motion records with a damping ratio of 5 percent. As shown in *Fig. 7*, since the average response spectrum is greater than the considered target design spectrum, the scale factor is taken as "1" for all earthquake records satisfying the criteria specified by TBEC-2018. Therefore, original ground motion records are employed in the analyses without interfering with their content.

5. ANALYSIS RESULTS AND DISCUSSION

Nonlinear response history analyses are performed for four numerical models using the selected 11 earthquake ground motion records. Four numerical models are composed of two individual numerical models of 4-story and 7-story buildings termed as "reference", pounding model of the existing adjacent buildings termed as "non-retrofitted", and finally pounding model of the retrofitted adjacent buildings termed as "retrofitted". Pounding forces, peak floor accelerations, inter-story drift ratios, and story shear force distributions obtained from the nonlinear time history analysis are recorded. The response of the original buildings and retrofitted buildings with steel columns are compared based on the selected engineering demand parameters. Comparisons are made for the average results of the selected 11 ground motion records for each of the numerical models. Plastic hinge distribution caused by the pounding effects of both buildings is also investigated for a specific ground motion record.

5.1. Pounding Forces

When the specified gap between the two buildings closes, the stiffness of the link elements activate and pounding forces develop in the link elements. Thus, the time and the pounding force can be determined for each link element when the collision occurs. Fig. 8 shows the variation of the pounding forces in both retrofitted and non-retrofitted models for the two ground motion records. In the retrofitted model, collision occurred at each floor in all earthquake ground motion records. Pounding took place only on the steel columns. There was no collision in the existing RC columns. The pounding-induced demands were prevented from being accumulated at a specific floor level by distributing the pounding effects throughout the building height by the applied retrofitting technique. As a result, a relatively more uniform distribution of pounding-induced seismic effects is ensured throughout the floors of the retrofitted building compared to the non-retrofitted one. Pounding forces reduce at the lower floors of the retrofitted building as a result of the decreasing displacement demands at the lower stories. The pounding forces are much greater in the non-retrofitted building. On the fourth floor of non-retrofitted building, pounding force was 3.13 times greater for Imperial Valley Earthquake record. The largest pounding forces took place on the fourth floor of both retrofitted and non-retrofitted buildings for Superstition Hills Earthquake record, which are almost the same. Seismic damage, on the other hand, is mostly localized in the fourth floor of the non-retrofitted building, resulting in brittle type shear failure in existing RC columns.

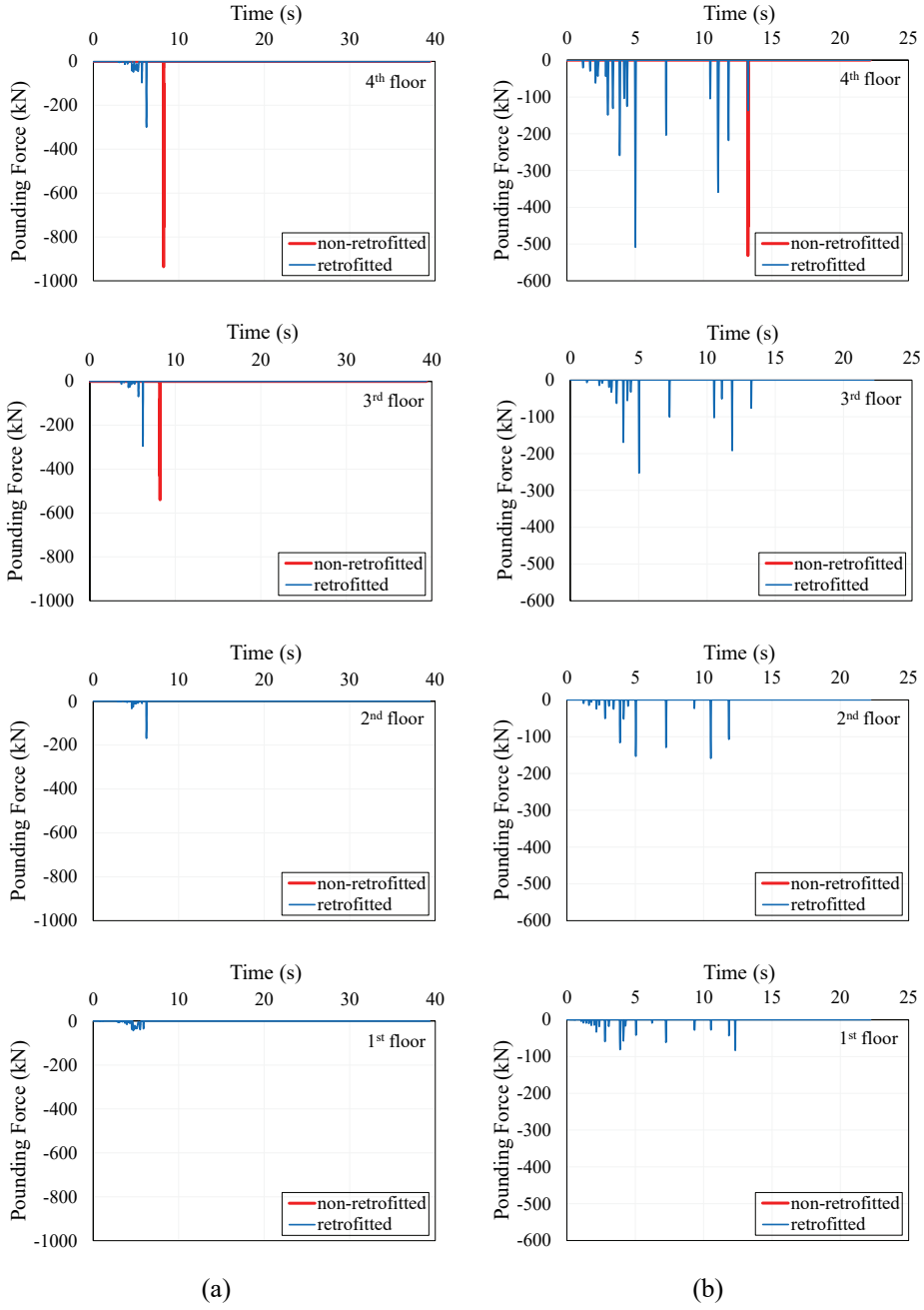

Fig. 8 - Variation of pounding forces at each floor (a) for Imperial Valley Earthquake record (Array #5), (b) for Superstition Hills Earthquake record.

5.2. Peak Floor Accelerations

Peak floor acceleration is an important engineering demand parameter for the safety of the building's contents and the comfort of its residents [55]. Peak floor acceleration values provide information about the seismic forces that will impose on the structural and nonstructural components. Fig. 9 shows the average peak acceleration values at each floor for all pounding models. For both buildings, pounding increases the floor accelerations at each floor. In 4-story building, the maximum average peak floor acceleration values of pounding models occurred in fourth floor of the building due to larger displacements. The maximum peak floor acceleration in retrofitted building is less than that in non-retrofitted building. In 4-story building, the maximum peak floor acceleration of the retrofitted and non-retrofitted building is 1.72 and 2.08 times larger than the reference building, respectively. In 7-story building, the maximum peak floor acceleration of the retrofitted and non-retrofitted building is 1.69 and 1.94 times larger than the reference building, respectively. In general, the pounding takes place in all floors of the retrofitted buildings. However, in non-retrofitted buildings, the pounding localized mostly in a single floor where the pounding first takes place. Because the pounding demands are distributed throughout the retrofitted models rather than localized in one floor as in the case of non-retrofitted building, the floor accelerations of retrofitted building are lower than the ones for non-retrofitted building. There is a jump even in the average peak floor accelerations at the fourth floor of both 4-story and 7-story non-retrofitted buildings. As also observed in the pounding force variations in *Fig. 8*, pounding took place mostly in the fourth floor only for the non-retrofitted building. This caused the localization of pounding effects at the fourth floor of both non-retrofitted buildings. On the other hand, as the pounding occurred in all floors of the retrofitted models, there is no distinct jump in the average peak floor acceleration values.

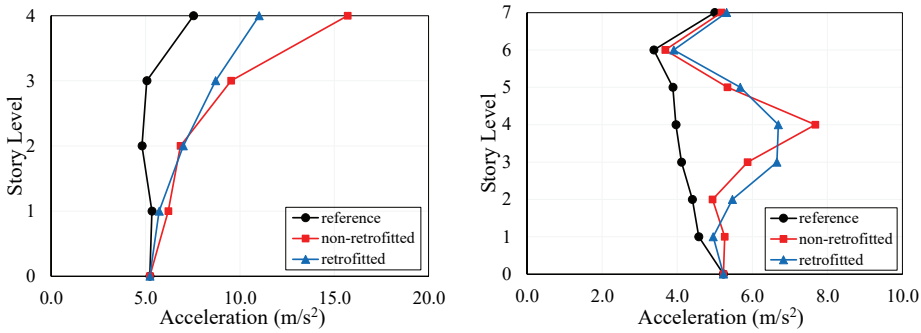

Fig. 9 - Average peak floor accelerations for buildings (a) 4-story, (b) 7-story.

5.3. Inter-Story Drift Ratios

Inter-story drift ratio (ISDR), a fundamental indicator for seismic damage for structural and non-structural components, plays a critical role in structural performance. During an earthquake, if the ISDR is excessive, both structural and non-structural components will be damaged. Thus, the ISDR is restricted to a certain limit in building design codes in order to

protect the components of the buildings. Fig. 10 shows the variation of ISDR in 4- and 7-story buildings.

The effect of pounding on the variation of ISDR is not as pronounced as in the case of peak floor acceleration distribution. Compared to the reference 4-story building, the maximum increase in ISDRs at the fourth story of the retrofitted 4-story building is 21.8 percent, while it is 15.4 percent at the fourth story of the non-retrofitted 4-story building. Compared to the reference 7-story building, the maximum increase in ISDRs at the sixth story of the retrofitted 7-story building is 27.6 percent, while it is 15.0 percent at the sixth story of the non-retrofitted 7-story building. In retrofitted buildings, the increase in ISDR values is greater. Since pounding did not cause any brittle type of shear failure to the columns of the retrofitted building, retrofitted building has more ductile behaviour and has more displacement capacity for additional displacement demands.

The maximum increase in ISDR occurs on the sixth story level of the 7-story building and the fourth story level of the 4-story building. When buildings collide, the floors below the fourth floor, where the pounding takes place, of the 7-story building have reduced ISDR than the reference building. The 4-story building reduces the displacement of the first 4 floors of the 7-story building. However, the floors above the pounding floor of the 7-story building displaced more by the impact of the post-collision. Thus, for the 7-story building, there is an increase in ISDRs at the floors above the pounding floor whereas the ISDRs are reduced in the floors below the pounding floor. This response is clearly observed in *Fig. 10*(b) referred as the whiplash effect, which causes changes in the displacements below and above the pounding floor [2,11,56]. On the other hand, ISDR of the 4-story reference building is less than the others when the pounding takes place. In both 4-story and 7-story buildings, the retrofitted buildings have increased ISDR values at each story than the non-retrofitted buildings. When the brittle type of RC column shear failure is prevented by the introduction of steel columns for retrofitting purposes, the overall behaviour mode of the buildings is dominated by the flexural response of the columns.

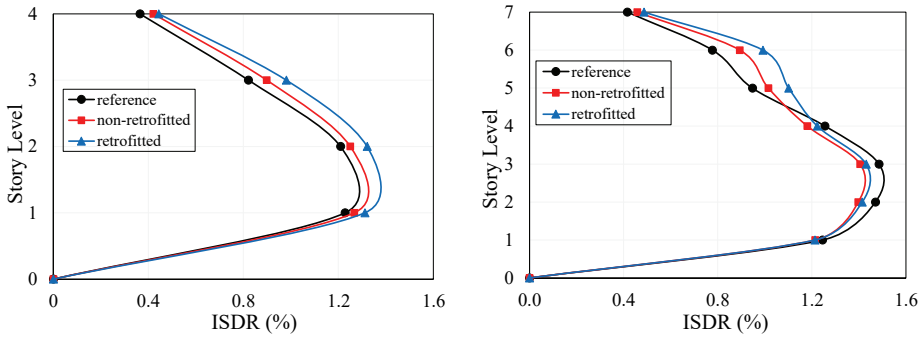

Fig. 10 - Average ISDR distribution for buildings (a) 4-story, (b) 7-story.

5.4. Story Shear Force

Maximum story shear force distributions are given in *Fig. 11* for the two buildings. The presented average values are the peak value of the sum of the shear forces in the vertical structural elements at each story under each earthquake record. The increase in the story shear force is evident at the stories above and below the pounding level. In the 7-story building, the increase in the shear forces at the floor above the pounding elevation is obvious due to whiplash effect. The maximum increase in the story shear force of the retrofitted 4-story building is 36.2 percent at the fourth story, while it is 43.6 percent in the non-retrofitted 4-story building. The maximum increase in the story shear force of the retrofitted 7-story building is 22.2 percent at the fifth story, while it is 13.2 percent in the non-retrofitted 7-story building. Story shear forces have increased in retrofitted buildings. This is due to the fact that pounding has not caused shear damage to existing RC columns with the addition of steel columns for retrofitting purposes. Thus, the displacement of the columns increases so does the shear force demands in the columns.

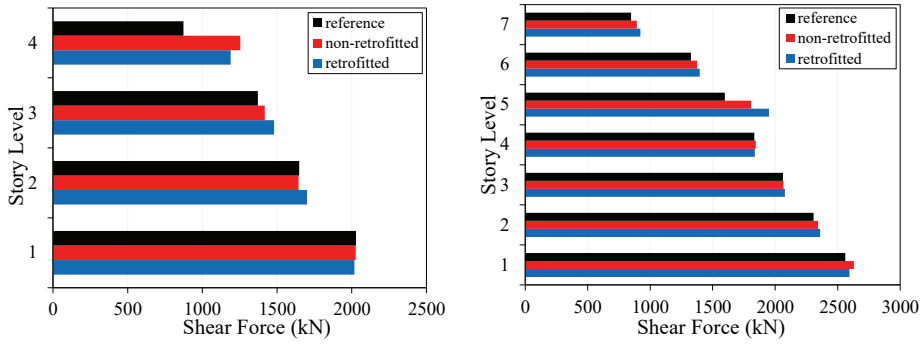

Fig. 11 - Average story shear force distributions for the buildings (a) 4-story, (b) 7-story.

5.5. Plastic Hinge Distributions

Plastic hinge distribution is examined under the Erzincan Earthquake ground motion record where the greatest pounding force occurs among the other selected records. Plastic hinge distributions of the buildings are presented in Fig. 12. Damage state of the assigned plastic hinges is determined according to the colored scale shown on the right side of Fig. 12. On the colored scale, “B” is the beginning of nonlinear behaviour and “E” is the ultimate point, beyond which the member failure takes place. (IO) corresponds to the limited damage, (LS) corresponds to the significant damage, and (CP) corresponds to collapse prevention limit states in TBEC-2018. Pounding significantly changes the plastic hinge distribution of both buildings. There is an increase in the number of damaged column and beam members at the upper floors of the buildings after pounding.

When Fig. 12 (b) and (c) are compared with Fig. 12 (a), it is observed that the plastic rotation demands in ground story beams and columns of 4-story building have increased, whereas the plastic rotation demands in ground story beams and columns of 7-story building have decreased. This result is consistent with the fact that pounding causes an increase in the

ISDRs of 4-story building and a decrease in the ISDRs of a 7-story building below the pounding floor as shown in Fig. 10.

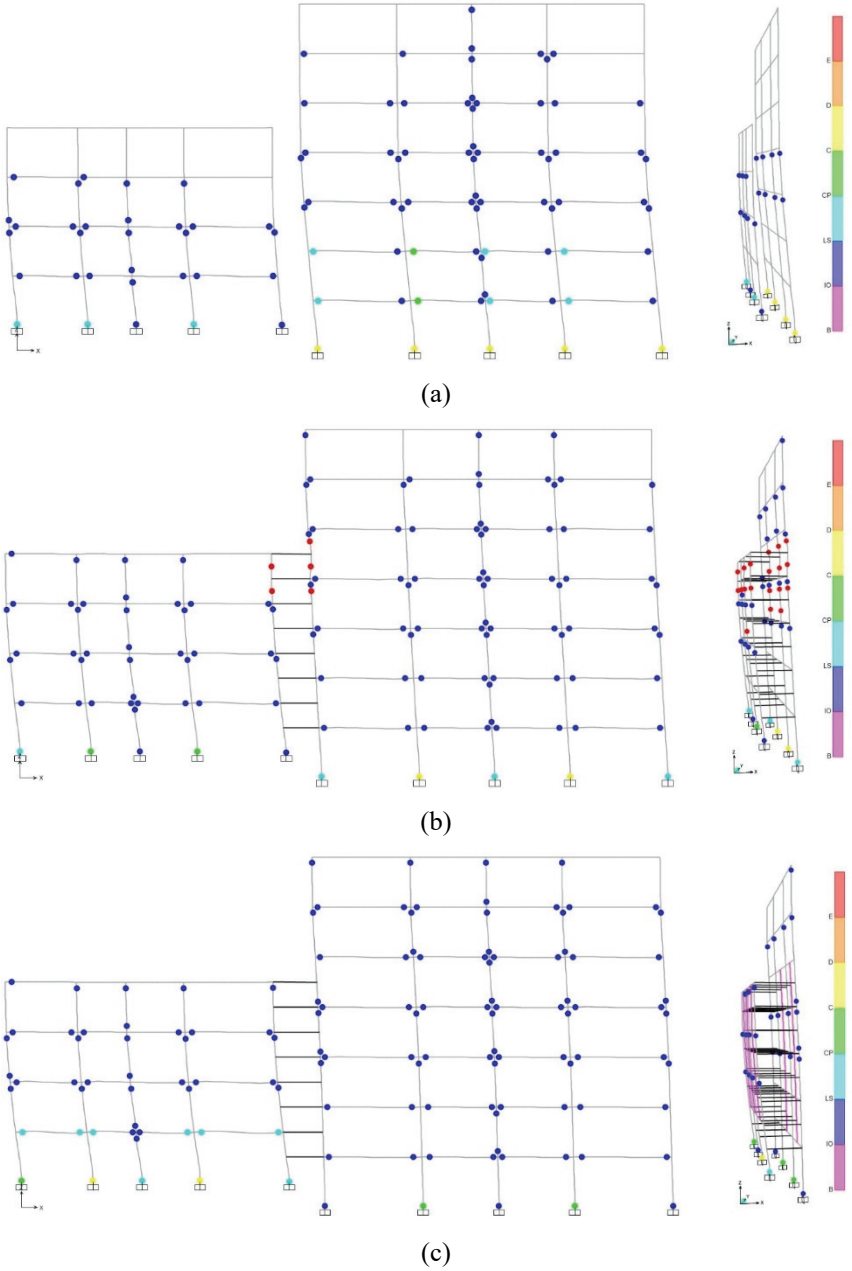

Fig. 12 - Plastic hinge distribution for the Erzincan Earthquake record (a) reference buildings, (b) non-retrofitted buildings, (c) retrofitted buildings.

As shown in Fig. 12 (b), shear failure in several columns of the non-retrofitted buildings has been observed at the stories where pounding takes place. In the retrofitted building, although the pounding takes place in each story, no shear failure is observed in the added steel columns or in the existing RC columns. Therefore, by introducing steel columns for retrofitting purposes, the existing RC columns are protected from any brittle type of shear failure. This leads to more ductile behaviour with increased ISDRs, and plastic rotation demands in the lower stories. Therefore, the detrimental effects of collision between adjacent buildings are minimized and the overall seismic response of the buildings is improved by eliminating the column shear failures.

6. CONCLUSIONS

In this paper, the effectiveness of the proposed retrofitting strategy for protecting existing RC columns against pounding effects has been investigated. Firstly, 3D numerical models of the 4- and 7-story RC buildings representing the existing building stock are developed in SAP2000 program. Then, steel columns with neoprene rubber pads were introduced in the retrofitted buildings. Nonlinear time-history analyses were conducted with 11 different real ground-motion records. The variations in pounding force, peak floor accelerations, ISDRs, story shear forces, plastic hinge distributions are examined for all pounding cases. The analysis results for each engineering demand parameter are compared for reference buildings, non-retrofitted buildings, and retrofitted buildings. Following conclusions were drawn based on the results of this study:

- With the introduction of steel columns in retrofitted buildings, pounding takes place in each story with reduced pounding forces. This enables a relatively more uniform distribution in the pounding-induced seismic effects along the height of the building. Whereas, in the non- retrofitted building, pounding forces are much larger and the seismic damage is mostly localized in the pounding story causing brittle type of shear failure in RC columns.
- The peak floor accelerations are observed to be increased due to pounding. The increase in peak accelerations at floors with larger displacements is especially pronounced as a result of pounding. Because pounding demands are distributed throughout the retrofitted building, the increase in peak floor accelerations is less in retrofitted buildings compared to the non-retrofitted buildings. Distinct jumps in the average peak floor accelerations were observed in the non-retrofitted building as a result of localization of pounding in a single floor.
- The variation in the ISDR is not as significantly affected by pounding as it is in the case of peak floor accelerations. There is an increase in the ISDR of 4-story building with pounding. Because of the change in the dynamic response of the 7-story building, ISDRs have increased at floors above the fourth story, at which the pounding takes place. However, in the lower stories of the 7-story building, ISDRs have decreased due to pounding with the 4-story building.
- Story shear forces have been increased due to pounding. There is greater increase, particularly in the retrofitted building because the existing columns could resist more lateral force without shear damage. The largest increase of shear forces took place in

the pounding stories, which are the roof story of the 4-story building and the fifth story of the 7-story building.

- The distribution of plastic hinges is one of the most significant indicators for the effectiveness of the proposed retrofitting strategy against pounding. Pounding caused a significant change in the damage profile of the buildings with an increase in the number of damaged members. The shear capacity of RC columns in the non-retrofitted buildings was exceeded during collision, and shear failure was observed in several columns at the pounding elevation. The existing RC columns in the retrofitted building did not exhaust their shear capacity because no collision occurred in existing RC columns. Thus, pounding impact spread throughout the structural members. The proposed retrofitting method protects the existing RC columns from brittle type of shear failure as a result of pounding.

The results are valid only for the 4- and 7-storey buildings used in this study. The retrofitting method can be used by extending the findings to other buildings. Future studies can be extended to investigate the effectiveness of the proposed retrofitting approach for the adjacent buildings at which the collision can take place at different column elevations rather than the column mid-point as is the case in this paper.

Acknowledgments

This work was supported by The Scientific and Technological Research Council of Turkey (TÜBİTAK) [grant number 120M877]

References

[1] Maison BF, Kasai K. Analysis for a Type of Structural Pounding. J Struct Eng 1990; 116(4):957–77.

[2] Anagnostopoulos SA, Spiliopoulos KV. An investigation of earthquake induced pounding between adjacent buildings. Earthq Eng Struct Dyn 1992;21:289–302.

[3] TBEC-2018. Turkish Building Earthquake Code. Ankara, Turkey: 2018.

[4] Jeng V, Kasai K, Maison BF. A Spectral Difference Method to Estimate Building Separations to Avoid Pounding. Earthq Spectra 1992;8:201–23. https://doi.org/10.1193/1.1585679.

[5] Kamal M, Inel M. Simplified approaches for estimation of required seismic separation distance between adjacent reinforced concrete buildings. Eng Struct 2021:113610. https://doi.org/10.1016/j.engstruct.2021.113610.

[6] Favvata MJ. Minimum required separation gap for adjacent RC frames with potential inter-story seismic pounding. Eng Struct 2017;152:643–59. https://doi.org/10.1016/j.engstruct.2017.09.025.

[7] Kamal M, Code-based new approaches for determining the minimum required separation gap. Structures 2022;46:750-764. https://doi.org/10.1016/j.istruc.2022.10.075.

[8] Khatami SM, Naderpour H, Razavi SMN, Barros RC, Sołtysik B, Jankowski R. An ANN-Based Approach for Prediction of Sufficient Seismic Gap between Adjacent Buildings Prone to Earthquake-Induced Pounding. Applied Sciences 2020;10:3591. https://doi.org/10.3390/app10103591.

[9] Khatami SM, Naderpour H, Barros RC, Jankowski R. Verification of Formulas for Periods of Adjacent Buildings Used to Assess Minimum Separation Gap Preventing Structural Pounding during Earthquakes. Advances in Civil Engineering 2019:1–8. https://doi.org/10.1155/2019/9714939.

[10] Anagnostopoulos S. Building pounding Re-examined: How Serious a Problem Is It? Elev World Conf Earthq Eng Acapulco, Mex June 23-28, 1996 1996:Paper 2108.

[11] Karayannis CG, Favvata MJ. Earthquake-induced interaction between adjacent reinforced concrete structures with non-equal heights. Earthq Eng Struct Dyn 2005;34:1–20. https://doi.org/10.1002/eqe.398.

[12] Karayannis CG, Naoum MC. Torsional behavior of multistory RC frame structures due to asymmetric seismic interaction. Eng Struct 2018;163:93–111. https://doi.org/10.1016/j.engstruct.2018.02.038.

[13] Korkmaz SZ. Observations on the Van Earthquake and Structural Failures. J Perform Constr Facil 2015;29:04014033. https://doi.org/10.1061/(ASCE)CF.1943-5509.0000456.

[14] Rosenblueth E, Meli R. The 1985 Earthquake: Causes and Effects in Mexico City. Concr Int 1986;8(5):23–34.

[15] Kasai K, Maison BF. Building pounding damage during the 1989 Loma Prieta earthquake. Eng Struct 1997;19:195–207. https://doi.org/10.1016/S0141-0296(96)00082-X.

[16] Youd TL, Bardet JP, Bray JD. Kocaeli, Turkey, earthquake of August 17, 1999. Oakland, California: Earthquake Engineering Research Institute; 2000.

[17] Yurdakul Ö, Duran B, Tunaboyu O, Avşar Ö. Field reconnaissance on seismic performance of RC buildings after the January 24, 2020 Elazığ-Sivrice earthquake. Nat Hazards 2021;105:859–87. https://doi.org/10.1007/s11069-020-04340-x.

[18] Inel M, Ozmen HB, Akyol E. Observations on the building damages after 19 May 2011 Simav (Turkey) earthquake. Bull Earthq Eng 2013;11:255–83.

[19] Sharma K, Deng L, Noguez CC. Field investigation on the performance of building structures during the April 25, 2015, Gorkha earthquake in Nepal. Eng Struct 2016;121:61–74. https://doi.org/10.1016/j.engstruct.2016.04.043.

[20] Cole GL, Dhakal RP, Turner FM. Building pounding damage observed in the 2011 Christchurch earthquake. Earthq Eng Struct Dyn 2012;41:893–913. https://doi.org/10.1002/eqe.1164.

[21] Romão X, Costa AA,a , Paupério E, Rodrigues H, Vicente R, Varum H, Costa A. Field observations and interpretation of the structural performance of constructions after the 11 May 2011 Lorca earthquake. Eng. Fail. Anal. 2013;34:670-692. https://doi.org/10.1016/j.engfailanal.2013.01.040.

[22] Papadrakakis M, Mouzakis HP. Earthquake simulator testing of pounding between adjacent buildings. Earthq Eng Struct Dyn 1995;24:811–34. https://doi.org/10.1002/eqe.4290240604.

[23] Filiatrault A, Wagner P, Cherry S. Analytical prediction of experimental building pounding. Earthq Eng Struct Dyn 1995;24:1131–54. https://doi.org/10.1002/eqe.4290240807.

[24] Chau KT, Wei XX, Guo X, Shen CY. Experimental and theoretical simulations of seismic poundings between two adjacent structures. Earthq Eng Struct Dyn 2003;32:537–54. https://doi.org/10.1002/eqe.231.

[25] Jankowski R. Earthquake-induced pounding between equal height buildings with substantially different dynamic properties. Eng Struct 2008;30:2818–29.

[26] Inel M, Cayci T, Kamal M, Altınel O. Structural Pounding of Mid-Rise RC Buildings During Earthquakes, Proceedings of the second European conference on earthquake engineering and semiology; 2014.

[27] Raheem SA, Fooly MY, Shafy AA, Abbas YA, Omar M, Latif MMSA, Mahmoud S. Seismic pounding effects on adjacent buildings in series with different alignment configurations. Steel and Composite Structures 2018;28(3):289-308.

[28] Raheem SEA, Fooly MY, Omar M, Zaher AKA. Seismic pounding effects on the adjacent symmetric buildings with eccentric alignment. Earthq Struct 2019;16(6):715-726.

[29] Raheem SEA, Alazrak T, AbdelShafy AG, Ahmed MM, Gamal YA. Seismic pounding between adjacent buildings considering soil-structure interaction. Earthquakes and Structures 2021;20(1): 55-70.

[30] Anagnostopoulos SA. Pounding of buildings in series during earthquakes. Earthq Eng Struct Dyn 1988;16:443–56.

[31] Rezavandi A, Moghadam AS. Experimental and Numerical Study on Pounding Effects and Mitigation Techniques for Adjacent Structures. Adv Struct Eng 2007;10:121–34. https://doi.org/10.1260/136943307780429752.

[32] Polycarpou PC, Komodromos P, Polycarpou AC. A nonlinear impact model for simulating the use of rubber shock absorbers for mitigation the effect of structural pounding during earthquakes. Earthq Eng Struct Dyn 2013;42:81–100. https://doi.org/10.1002/eqe.

[33] Sołtysik B, Falborski T, Jankowski R. Preventing of earthquake-induced pounding between steel structures by using polymer elements-experimental study. Procedia Eng 2017;199:278–83. https://doi.org/10.1016/j.proeng.2017.09.029.

[34] He J, Jiang Y, Xue Q, Zhang C, Zhang J. Effectiveness of Using Polymer Bumpers to Mitigate Earthquake-Induced Pounding between Buildings of Unequal Heights. Adv Civ Eng 2018;2018:1–14.

[35] Raheem SEA. Mitigation measures for earthquake induced pounding effects on seismic performance of adjacent buildings. Bull Earthquake Eng 2014;12:1705–1724. https://doi.org/10.1007/s10518-014-9592-2.

[36] Anagnostopoulos SA, Karamaneas CE. Use of collision shear walls to minimize seismic separation and to protect adjacent buildings from collapse due to earthquake-induced pounding. Earthq Eng Struct Dyn 2008;37:1371–88.

[37] N.K. A, Neeraja N. Evaluation of Seismic Pounding between Adjacent Buildings. Int J Innov Res Sci Technol IJIRST 2016;3:138–47. https://doi.org/10.15224/978-1-63248-105-4-24.

[38] Noman M, Alam B, Fahad M, Shahzada K, Kamal M. Effects of pounding on adjacent buildings of varying heights during earthquake in Pakistan. Cogent Eng 2016;3:1225878. https://doi.org/10.1080/23311916.2016.1225878.

[39] Jankowski R, Mahmoud S. Linking of adjacent three-storey buildings for mitigation of structural pounding during earthquakes. Bull Earthq Eng 2016;14:3075–97. https://doi.org/10.1007/s10518-016-9946-z.

[40] Abdel-Mooty MAN, Ahmed NZ. Pounding Mitigation in Buildings using Localized Interconnections. Adv Struct Eng Mech (ASEM17), 28 August-1 Seprember, 2017, Ilsan (Seoul), Korea 2017.

[41] Nishath PV, Abhilash PP. Mid-Column Pounding Effects On Adjacent Tall Buildings and Its Mitigation Using Viscous Dampers and Friction Dampers. Int J Sci Eng Res 2017;8:168–73.

[42] Pargoo NS, Hejazi F, Jabbar S. Preventing Seismic Pounding of Adjacent Structures Using Viscous Wall Damper Device. GCEC 2017 Proc. 1st Glob. Civ. Eng. Conf., 2019, p. 561–77. https://doi.org/10.1007/978-981-10-8016-6_44.

[43] Inel M, Ozmen HB, Şenel ŞM, Kayhan AH. Mevcut Betonarme Binaların Yapısal Özelliklerinin Belirlenmesi. International Earthquake Symposium of Sakarya, Turkey 2009 [in Turkish].

[44] SAP2000. Integrated Finite Element Analysis and Design of Structures. Bekeley (CA, USA): Computer and Structures Ins.

[45] Mander JB, Priestley MJN, Park R. Theoretical Stress-Strain Model for Confined Concrete. J Struct Eng 1988;114:1804–25.

[46] XTRACT. Cross Sectional Analysis of Components, Imbsen Software System. Sacramento.

[47] Çelik Yapıların Tasarım, Hesap ve Yapım Esaslarına Dair Yönetmelik. Ministry of Environment and Urban Planning, Ankara, Turkey 2018.

[48] Anagnostopoulos SA. Equivalent viscous damping for modeling inelastic impacts in earthquake pounding problems. Earthq Eng Struct Dyn 2004;33:897–902. https://doi.org/10.1002/eqe.377.

[49] Jankowski R. Non-linear viscoelastic modelling of earthquake-induced structural pounding. Earthq Eng Struct Dyn 2005;34:595–611. https://doi.org/10.1002/eqe.434.

[50] Muthukumar S, DesRoches R. A Hertz contact model with non-linear damping for pounding simulation. Earthq Eng Struct Dyn 2006;35:811–28. https://doi.org/10.1002/eqe.557.

[51] Naserkhaki S, Abdul Aziz FNA, Pourmohammad H. Parametric study on earthquake induced pounding between adjacent buildings. Struct Eng Mech 2012;43:503–26. https://doi.org/http://dx.doi.org/10.12989/sem.2012.43.4.503503.

[52] Jameel M, Saiful Islam ABM, Hussain RR, Hasan SD, Khaleel M. Non-linear FEM analysis of seismic induced pounding between neighbouring Multi-storey Structures. Lat Am J Solids Struct 2013;10:921–39.

[53] Altınel O. Investigation of Pounding Effects on Seismic Performance of Existing Sequential Buildings. MSc Thesis. Pamukkale University. Denizli, Turkey 2015 [in Turkish]

[54] Naeim F, Kelly JM. Design of seismic isolated structures: from theory to practice. John Wiley & Sons, Inc; 1999.

[55] Çerçevik AE, Avşar Ö, Dilsiz A. Optimal Placement of Viscous Wall Dampers in RC Moment Resisting Frames Using Metaheuristic Search Methods. Engineering Structures 2021;249:113108. https://doi.org/10.1016/j.engstruct.2021.113108.

[56] Naserkhaki S, El-Rich M, Abdul Aziz FNA, Pourmohammad H. Pounding between adjacent buildings of varying height coupled through soil. Struct Eng Mech 2014;52:573–93. https://doi.org/10.12989/sem.2014.52.3.573.